Research Square

Preprints are preliminary reports that have not undergone peer review.
They should not be considered conclusive, used to inform clinical practice,
or referenced by the media as validated information.

Chemisorptive and synergistic bioremediation of arsenic from wastewater using bacterial consortia: mechanistic insights and surface characterization

Arpita Chakraborty
Swami Vivekananda University
Samudra Pal
Swami Vivekananda University
Tuhin Mukherjee
Swami Vivekananda University
Tanya Das
Swami Vivekananda University
Nimai Chandra Saha
Harichand Guruchand University
Palash Kumar Pal
palashkp@svu.ac.in

Swami Vivekananda University

Research Article

Keywords: Arsenic, Bacterial consortia, Bioremediation, Scanning electron microscopy, Atomic absorption spectroscopy, Fourier-transform infrared spectroscopy

Posted Date: June 5th, 2026

DOI: https://doi.org/10.21203/rs.3.rs-9860438/v1

License: This work is licensed under a Creative Commons Attribution 4.0 International License.
Read Full License

Additional Declarations: No competing interests reported.

Abstract

Arsenic (As) contamination in aquatic environments and its mobilization in wastewater pose significant threats to ecosystem integrity and human health. This study evaluated the bioremediation potential of three arsenic-resistant bacterial strains (C2, C4, and C5) isolated from heavy metal-contaminated agricultural water and their binary consortia (C2C4, C2C5, and C4C5) as eco-friendly and cost-effective remediation solutions. Molecular identification via 16S rRNA gene sequencing characterized the isolates as *Bacillus* sp. (C2), *Bacillus pumilus* (C4), and *Fictibacillus phosphorivorans* (C5). Physiological characterization revealed optimal growth at pH 7.0 and 35°C, with thermotolerance up to 75°C. Morphological and biochemical analyses confirmed Gram-positive and rod-shaped cellular morphology. Antibiotic susceptibility profiling demonstrated high sensitivity to ciprofloxacin, moderate susceptibility to azithromycin (C2 > C4 > C5), and variable resistance to cephalosporins, with all strains susceptible to ampicillin. Arsenic tolerance assays across 5-200 ppm concentrations of As(III) and As(V) established a minimum inhibitory concentration of 50 mg/L for both oxidation states, achieving > 50% removal efficiency. Scanning electron microscopy established successful consortium formation and revealed their phenotypic adaptations under arsenic stress. Fourier-transform infrared spectroscopy indicated alterations of the functional groups in bacterial cell walls as metabolic adjustments in response to arsenic toxicity. Atomic absorption spectroscopy indicated superior bioremediation capacity of the bacterial consortia (78–85%) in comparison to the individual isolates (60–65%). Collectively, it appears that the formed bacterial consortia, through synergistic microbial interactions, can deliver better bioremediation of arsenic from wastewater, reinforcing the ecological and biotechnological relevance of arsenic-resistant bacteria as sustainable, cost-effective alternatives to conventional remediation methods.

1. INTRODUCTION

Heavy metal contamination of soil and water from both anthropogenic and geogenic sources has significantly increased in current days. Major reasons of this disaster are due to rapid population growth, industrialization, urbanization, and intensive agricultural practices (Adetunji et al., 2023). Among these pollutants, arsenic (As), which is considered as a very poisonous and persistent metalloid, has become a major global environmental and public health concern. There are 70 countries in which arsenic has a significant effect on human health (Aliyari Rad et al., 2023). It is noted that there are 14 states in India that are severely affected by arsenic, particularly the state of West Bengal (Aluko et al., 2021). Surprisingly, the major source of arsenic found in the Bengal Basin is the Ganges-Brahmaputra-Meghna river system. With increased pollution of surface waters in the 1970s, large masses of people were forced to use groundwater, thus unwittingly putting millions at risk of arsenic poisoning (Alves et al., 2022).

Arsenic exists in several different forms in the environment, including arsine (As^{-3}), elemental arsenic (As^{0}), arsenite (As^{3+}), and arsenate (As^{5+}), all of which are highly toxic substances that harm living organisms. As an analogue of phosphate, arsenate is able to enter the organism through phosphate

transporters and affect essential biological processes like phosphorylation and ATP generation (Arce-Inga et al., 2022). Consumption of water containing elevated levels of arsenic (greater than the permissible limit (50 µg/L)) can adversely affect health, causing conditions such as skin ulcers, hyperpigmentation, hepatosplenomegaly, nervous system malfunctioning, and skin cancer. The health effects also include bladder, lung, and gastrointestinal cancers (Praveen et al., 2022). Even low concentrations of arsenic can negatively impact physiology and metabolism. Arsenic remains present in the environment due to its high solubility, complicating the removal process from polluted areas. Conventional treatment procedures such as chemical precipitation and adsorption are economically unfeasible, energy-intensive, and environmentally hazardous (Bertin et al., 2022; Shah et al., 2022).

In this regard, arsenic-resistant bacteria have received considerable focus because of their capability of thriving in the presence of arsenic due to diverse mechanisms of detoxification, including oxidation-reduction reactions, methylation, sequestration, adsorption, chelation, and efflux systems. Different biomolecules such as polysaccharides, proteins, and lipids are released by bacterial cells, which get associated with the heavy metal. In this way, the bioavailability of arsenic gets reduced and its toxicity diminishes (Bhatt et al., 2023). Microbial bioremediation of arsenic contamination is now being appreciated as an economical and environmentally friendly approach. Not only do bacteria reduce the toxicity of arsenic but they also make soil fertile and optimize physical and chemical properties of the soil. Knowledge about the molecular mechanisms underlying arsenic resistance in microorganisms will facilitate the development of innovative approaches for the reduction of arsenic contamination.

The findings of the current study demonstrated extremely high levels of arsenic contamination in the pond water of Dhapa, West Bengal, where the level of arsenic contamination was higher than 10 µg/L, which is the limit set by WHO. The research focuses on the isolation and characterization of indigenous arsenic-resistant bacterial strains capable of tolerating high concentrations of both As(III) and As(V) (Doane et al., 2020). The minimal inhibitory concentration (MIC) and growth kinetics of the isolates were analyzed using UV-Visible spectroscopy, while biochemical assays were conducted for phenotypic characterization. 16S rRNA gene sequencing was used for molecular identification followed by Fourier-transform infrared (FTIR) spectroscopy to identify functional groups associated with arsenic stress responses (Darma et al., 2022; Dey et al., 2024; Roy et al., 2024). Moreover, scanning electron microscopy (SEM) was used to detect the changes in the bacterial morphology, and finally, atomic absorption (AAS) study was conducted to evaluate the bioremediation potential of the bacteria. The findings aim to enhance understanding of microbial adaptations to arsenic toxicity and identify promising bacterial consortia for sustainable bioremediation of arsenic-contaminated soil and water systems (Praveen et al., 2022; Khandelwal et al., 2024; Naiel et al., 2024).

2. MATERIALS AND METHODS

2.1. Study Area:

Dhapa, a dumping zone located in the district of North 24 Parganas, West Bengal, India, has been reported earlier as a heavy metal, particularly arsenic, contaminated area (Das et al., 2014). Thus, soil and water samples were collected from this specific area located between 22°33'45.8" N and 88°25'12.4" E. The site experiences a tropical wet-and-dry weather with mean annual temperature of approximately 26°C. The maximum temperature (~ 39°C) occurs during summer, whereas the minimum (~ 14°C) is recorded in winter. The region receives substantial monsoonal rainfall from June to September, which plays a vital role in both waste leaching and agricultural practices. Geologically, the Dhapa area lies within the lower Ganges deltaic plain, primarily composed of recent alluvial deposits, including silt, clay, and fine sand layers. The accumulation of industrial and municipal solid waste in this zone contributes significantly to the enhanced levels of arsenic and other heavy metals detected in the surrounding soil and groundwater (Flores et al., 2022; Ghosh et al., 2024).

2.2. Collection of soil and water samples:

Water samples were collected from areas adjacent to the waste-impacted ponds and drainage channels (within 3–5 m proximity) using sterilized 500 mL glass bottles. Immediately after collection, samples were sealed, labeled, and placed in thermal containers to prevent contamination and degradation. A total of five water samples were collected from different locations across the site during the pre-monsoon season (May-June), representing the summer sampling period. All collected samples were stored at 4°C for subsequent physicochemical and microbial analyses, which were conducted within 24 hours of collection to ensure accuracy and reliability of results (Sher et al. 2023).

2.3. Chemicals and Reagents:

All culture media, including Nutrient Broth (NB), Nutrient Agar (NA), and Luria Bertani (LB), were obtained from HiMedia Laboratories Pvt. Ltd., Mumbai, India. The arsenic compounds used in this study- arsenic(III) as sodium arsenite ($NaAsO_2$) and arsenic(V) as sodium arsenate ($Na_2HAsO_4{\cdot}7H_2O$)- were also procured from HiMedia Laboratories, West Bengal, India. FTIR-grade ethanol and distilled water were supplied by Thermo-Fisher Scientific, while all other reagents were of analytical reagent (AR) grade, purchased from Merck India Ltd. All glassware used in the experiments were pre-cleaned by soaking in 15% nitric acid (HNO_3) and thoroughly rinsed with double-distilled water prior to use. All reagents and standard solutions of As(III) and As(V) were prepared using double-distilled water to ensure the accuracy and reliability of subsequent analyses.

2.4. Estimation of heavy metal concentration in wastewater samples:

Collected wastewater samples were investigated under controlled laboratory conditions. The concentrations of heavy metals (Table-1), including arsenic (As), lead (Pb), chromium (Cr), and cadmium (Cd), were quantified using Atomic Absorption Spectroscopy (AAS; Thermo Scientific; Model: iCE 3000 Series) following the method of Roy et al. (2017).

2.5. Isolation, media optimization and cultivation of bacterial strains:

In order to isolate distinct bacterial colonies, collected water samples were serially diluted in autoclaved distilled water to achieve successive dilutions up to 10^{-9}. Further, 0.1 mL aliquots from the 10^{-7} and 10^{-8} dilutions were spread onto Nutrient Agar (NA) plates containing peptone (0.5%), yeast extract (0.3%), NaCl (0.5%), glucose (0.25%), and agar (1.5%), with an adjusted pH 7.0. The plates were incubated at 37 ± 1°C for 24 h for appropriate colony formation. Based on the morphology, size, and pigmentation, specific colonies were selected. In order to collect and culture single colonies, they individually were sub-cultured onto separate NA slants by repeated streaking and incubated for 24 hours at the same temperature. In order to evaluate the growth performance, seven morphologically different bacterial isolates were cultured in 100 mL of Luria-Bertani (LB**)** and Nutrient Broth (NB) media. Growth kinetics of the bacterial isolates were monitored for 96 h by measuring the optical density (OD_{600} nm) using a spectrophotometer. Cultures in the mid-logarithmic phase were used for downstream experiments, while long-term preservation of the isolates was achieved in 20% (v/v) glycerol stocks at -80°C, ensuring viability and genetic stability (Roy et al., 2017).

2.6. Viable cell counts and identification of arsenic resistant bacteria:

The collected wastewater samples were serially diluted to isolate distinct bacterial colonies. Initially, 1 mL of the water sample was mixed with distilled water (autoclaved), and successive dilutions up to 10^{-9} were prepared under aseptic conditions. From the 10^{-7} dilution, 0.1 mL aliquots were spread on Nutrient Agar (NA) plates containing 0.5% peptone, 0.3% yeast extract, 0.5% NaCl, 0.25% glucose, and 1.5% agar at pH 7.0, followed by incubation at 37 ± 1°C for 24 hours. Distinct colonies (C1-C5) differing in size, shape, and color were purified through successive streaking on fresh NA slants and incubated for another 24 hours to obtain pure cultures.

In order to verify the arsenic resistance of the isolated bacterial strains (C1-C5), a viable cell count study was performed following standard methods (Roy et al., 2017). Each bacterial isolate was inoculated into NB supplemented (100 mg/L) with arsenate or arsenite and incubated for 72 hours. At 24-hour intervals, cultures were transferred accordingly onto NA plates supplemented with or without arsenic. The colony-forming units (CFUs) were counted after 24 hours of incubation to assess bacterial survival and tolerance. The isolates exhibiting consistent growth (C2, C4 and C5) in the presence of arsenic were considered arsenic-resistant and were maintained in LB and NB media for further physiological and biochemical characterization. Mid-log phase cultures were selected for subsequent assays, while long-term preservation was ensured by storing the strains in 20% (v/v) glycerol at -80°C.

2.7 16S rRNA-based bacterial identification and phylogenetic tree analysis:

Partial 16S-rRNA gene sequences of the bacterial isolates were analyzed for taxonomic identification by comparing them with bacterial and archaeal sequences available in the NCBI database using the BLAST tool (http://www.ncbi.nlm.nih.gov/blast). Sequences with over 99% similarity with the isolate were screened for further phylogenetic analysis. Following isolation of the genomic DNA from the selected bacterial isolates, expression of the 16S-rRNA gene was studied through PCR using universal primers (F: AGAGTTTGATCCTGGCTCAG; R: CGGTTACCTTGTTACGACTT). The amplified sequences were compared and analyzed using the BLAST-Nucleotide algorithm to search for similarity with known sequences in GenBank. The query sequences revealed 68–70% sequence similarity with the reference 16S-rRNA sequences from bacterial strains in the database. Thus, on the basis of resulting similarity matrix, a phylogenetic tree was postulated to determine the evolutionary relationships between the isolated strains and related sequences available in NCBI (Doane et al., 2020; Mohammad et al., 2022).

2.8 Determination of optimum pH and temperature:

In order to evaluate the influence of temperature and pH on bacterial growth, LB broth was used as the basal growth medium. Briefly, nine sterile test tubes with 10 mL of LB media in each were inoculated with 1 mL of freshly grown bacterial culture. First six cultures were incubated at 30°C, 35°C, 45°C, 55°C, 65°C, and 75°C for 24 h under both shaking and stationary conditions. In order to study the effect of pH, rest of the three cultures were subjected to different pH (5 or, 7 or, 9) adjusted with the help of HCl or NaOH and incubated at 37°C under continuous shaking for 24 hours. In either case, bacterial growth was quantified by measuring the optical density (OD_{600} nm) using a spectrophotometer (Roy et al., 2017; Bukhari et al., 2023; Mohammad et al., 2025).

2.9 Morphological and biochemical characterization:

Gram staining was performed to differentiate the bacterial isolates on the basis of their chemical and physical properties of their cell walls, specifically detecting the presence of peptidoglycan in Gram-positive bacteria (He et al., 2019). To assess physiological and metabolic capabilities, a set of selected biochemical tests was conducted following standard protocols (Dubey et al., 2012; Kaparwan et al., 2020). These included enzyme activity assays (catalase, oxidase, urease, and indole), methyl red, hydrogen sulfide (H_2S) production, sodium chloride tolerance, citrate utilization, and the ability to metabolize carbohydrates, starch, and lipids. Morphology of arsenic-resistant isolates were observed under a compound microscope at 100× magnification (LABOMED, LP Plan Acrho 9133040) to obtain further insights into cellular morphology and physiological traits. This provided detailed information on cell shape, surface texture, and external appendages, supplementing the biochemical and Gram staining results (Dubey et al., 2012; Kaparwan et al., 2020).

2.10 Antibiotic sensitivity test:

The antibiotic sensitivity of bacterial strains C2, C4, and C5 was evaluated through the zone of inhibition (ZOI) assay (Bertin et al., 2022), employing the antibiotics (10, 100, and 1000 mg/L) viz. kanamycin, azithromycin, ciprofloxacin, and ampicillin. Briefly, bacterial cultures were uniformly spread on agar plates, and antibiotic-impregnated discs were placed on the surface. After incubation, the diameters of

the clear zones surrounding the discs, where bacterial growth was restricted, were measured in millimeters using a calibrated scale (Bertin et al., 2022). These measurements provided a quantitative evaluation of each strain's susceptibility to the tested antibiotics, allowing comparison of relative sensitivity among the isolates. Strains exhibiting larger inhibition zones were considered highly sensitive, whereas smaller zones indicated lower susceptibility or resistance.

2.11 Preparation of bacterial consortia:

Selected bacterial isolates (C2, C4, and C5) were incubated independently in LB media at 37°C under continuous shaking for 24 hours until reaching the exponential growth phase to ensure maximum metabolic activity. The cultures were subsequently concentrated by adjusting the optical density (OD_{600}) to obtain uniform cell concentrations across all isolates. Following standardization, equal volumes (10 mL each containing about 1 g of bacteria) of the individual cultures were aseptically combined to establish the bacterial consortium (Lin et al., 2022). The resultant mixed culture was incubated in LB media at 37°C under continuous shaking for 24 hours to facilitate interspecies interaction and stabilization. The compatibility and synergistic potential of the consortium were preliminarily evaluated through growth dynamics by monitoring optical density (OD) at 600 nm over time.

2.12 Determination of Minimum Inhibitory Concentration (MIC):

In the present study, the minimum inhibitory concentration (MIC) of arsenic for each isolated bacterial strain and consortia was determined following the protocol described by Brown (2007**)**, with necessary modifications (Zhu et al., 2022). The isolates were inoculated into NB media supplemented with increasing concentrations of either sodium arsenite [As(III); 5, 10 and 20 mM] or, sodium arsenate [As(V); 50, 100 and 200 mM]. In addition, two separate inoculums containing either sodium arsenite or, sodium arsenate, respectively, devoid of any bacterial inoculation were maintained under identical conditions to ensure reliability. Cultures were incubated in a shaker incubator at 37 ± 1°C for 24 hours under aerobic conditions and the growth response of each bacterial strain was quantified in the same manner as described earlier. The lowest concentration showing no visible growth was recorded and considered as the MIC value for the respective particular strain (Rojas-Solis et al., 2023).

2.13 Topological study of the isolated arsenic-resistant bacteria through Scanning Electron Microscopy (SEM):

In order to investigate the alterations in the surface morphology and structural features of arsenic-resistant isolates and their consortia, samples were prepared and observed under a scanning electron microscope (SEM) at 15 kV (Zeiss; Gemini SEM 450) following well calibrated methods (Pandey et al., 2015; Merino et al., 2025) with little modifications. Briefly, after cultivating the bacterial isolates and their consortia at 30°C in LB broth, sodium arsenite [As(III); 5, 10 and 20 mM] or, sodium arsenate [As(V); 50, 100 and 200 mM] were supplemented in to it and maintained at the same temperature for 96 h. Following completion of the experiment, LB media containing bacteria was centrifuged at 5000 rpm for

15 mins room temperature. The suspended pellet was considered as crude bacterial sample. In order to remove the media, bacterial pellet was resuspended in PBS (50 mM; pH 7.2–7.4) and again centrifuged in the same manner. This process was continued for 2 more cycles to remove the media contamination that could interfere during the image processing of SEM. Now, the suspended bacteria were fixed in 4% v/v glutaraldehyde in PBS for 24 h at room temperature and then centrifuged at 5000 rpm for 15 mins room temperature and again washed in PBS once. After each one of the following dehydration steps, the bacterial samples were centrifuges in the same manner. Initially, the bacteria were treated with increasing gradient of ethanol (50–100% v/v) for 15 min each. After critical point drying in a pressurized chamber at a specific temperature (10°C), the bacterial samples were coated with Au 24 and observed under a SEM as mentioned above.

2.14 Fourier Transform Infrared Spectroscopy (FTIR) - based analysis of bacterial metabolites:

Fourier Transform Infrared Spectroscopy (FTIR) was employed to analyze alterations in functional groups and associated biomolecular signatures on the surface of bacterial cells (Ayangbenro et al., 2019; Fadlelmoula et al., 2022) before and after exposure to arsenic in its trivalent [As (III)] and pentavalent [As (V)] forms. The study was performed through a FTIR spectrometer (Lambda 365 Plus; PerkinElmer; Model: Spectrum Two). Briefly, fresh bacteria cultured for overnight were harvested by centrifugation (Thermo Scientific Sorvall ST8R) at 12,000 rpm for 5 minutes to collect sufficient biomass. The suspended cell pellets were washed three times in 0.5% NaCl to remove impurities and then dried in a hot air oven at 50°C for 8 hours to eliminate residual moisture. The dried biomass was finely ground using a mortar and pestle to prepare for analysis (Zeng et al., 2022). The resulting powder was scanned across a spectral range of 4000 to 500 cm^{-1} at a resolution of 4 cm^{-1}. Spectral data were recorded and analyzed using Spectrum IR software (version 10.7.2), enabling comparison of functional group variations between untreated and arsenic-treated bacterial cells (Kasprowicz et al., 2010; Faghihzadeh et al., 2016; Kepenek et al., 2019).

2.14 Evaluation of the arsenic bioremediation potential through Atomic Absorption Spectroscopy (AAS):

The isolated arsenic-resistant bacterial strains and their consortia were cultivated in LB broth to assess their ability to tolerate and remove arsenic from the medium. Three sets of cultures for each isolate or, consortia were prepared for arsenic (III) at concentrations of 5 ppm, 10 ppm, and 20 ppm (as sodium arsenite) and for arsenic (V) at 50 ppm, 100 ppm, and 200 ppm (as sodium arsenate). Each culture was prepared in 25 mL of LB broth in 50 mL conical flasks, and inoculated with 1 mL of actively growing bacterial suspension (~ 10^7 CFU/mL). All flasks were incubated in a shaker incubator at 37 ± 1°C with continuous agitation at 150 rpm to ensure adequate aeration. Control flasks containing the respective arsenic solutions (without bacterial inoculation) were maintained under identical conditions. At 96 hours, 10 mL aliquots of each culture were collected and centrifuged at 10,000 rpm for 10 minutes to separate the bacterial pellet from the supernatant. The arsenic concentration in the supernatant was then

quantified using AAS (Thermo Scientific; Model: iCE 3000 Series) following the standard procedures (APHA, 2017; Roy and Das, 2017). The reduction in arsenic concentration, in comparison to the control, over time was used to calculate the arsenic removal efficiency of the individual strains.

2.15 Statistical analysis:

All experimental data are expressed as mean ± SEM (standard error of the mean) of three independent replicates. Statistical significance in between the different experimental groups were evaluated by one-way analysis of variance (ANOVA) followed by a *post-hoc* Duncan's multiple range test (DMRT), considering $p < 0.05$ as the threshold of significance. Data representation was performed using GraphPad Prism software (version 8.0) and Microsoft Excel program.

3. RESULT

3.1 Isolation of arsenic resistant bacteria from wastewater and profiling of viable cells:

Following 96 h of incubation on LB agar amended with arsenic, several discrete colonies were observed. Among these, three isolates (designated as C2, C4, and C5) with pronounced growth during enrichment culture, were subjected to evaluation for detailed characterization and evaluation of their arsenic tolerance and remediation efficiency. Interestingly, subjecting the three isolates to arsenic exposure altered their growth behavior. Isolates grown on plates without arsenic exhibited a steady increase in growth up to 80 h, after which growth was restricted at 96 h (Fig. 1A; Supplementary file for Fig. 1). In contrast, on plates supplemented with sodium arsenate or arsenite, all the studied individual strains (C2, C4, and C5) and their consortium (C2C4, C2C5 and C4C5) continued to show an increase in viable cell counts (in terms of CFU mL^{-1}) up to 72 h.

3.2 Morphological characteristics and Gram staining of the isolates:

The colony characteristics of isolates varied in appearance from each other (Fig. 1A; Supplementary file for Fig. 1). In case of C2 (*Bacillus firmus*), the colonies were found to be rougher, larger, and more irregular with a comparatively dull coloration, forms small to medium-sized colonies that are circular, smooth, and convex with entire margins. The colony surface is usually glistening, and the color is creamy to off-white. However, colonies of isolate C4 (*Bacillus pumilus*) on nutrient agar were circular, smooth to slightly rough, opaque, and cream to off-white in color, with entire margins and a flat to slightly convex elevation (Fig. 1A). C5 (*Fictibacillus phosphorivorense*) showed smoother and more uniform colonies with a creamy appearance. Gram staining confirmed that all three isolates (C2, C4, and C5) were Gram-positive rod-shaped in nature (Fig. 1B).

3.3 Zone of inhibition indicated differential responses in the bacterial strains and their consortia:

Our results revealed that all the three bacterial strains (C2, C4 and C5) and their consortia (C2C4, C2C5 and C4C5) exhibited high sensitivity to both forms of arsenic (Fig. 1C; Supplementary file for Fig. 1), as evidenced by the expanding zones of inhibition with increasing concentrations of arsenic. Notably, the inhibition zones were larger for As(III) than for As(V) at higher concentrations, suggesting greater resistance of the strains to arsenate [As(V)] compared to arsenite [As(III)] (Fig. 1C).

3.4 Antibiotic sensitivity of the isolates:

The antibiotic susceptibility assay demonstrated variable inhibitory effects of different antibiotics against the bacterial strains C2, C4, and C5 at concentrations of 10, 100, and 1000 mg/L. Among the tested antibiotics, ciprofloxacin exhibited the strongest antibacterial activity, showing significant inhibition zones in both length and diameter measurements for all strains. At a concentration of 1000 mg/L, ciprofloxacin showed the strongest antibacterial effect, with strain C5 producing the largest inhibition zone diameter (5.5 cm), followed by C4 (3.6 cm) and C2 (3.4 cm). Noticeable inhibition was also observed at lower ciprofloxacin concentrations. Ampicillin exhibited weak activity and was effective only at 1000 mg/L, where strain C2 showed the highest inhibition length of 1.7 cm. Azithromycin demonstrated minimal inhibitory activity, with small inhibition zones mainly recorded at the highest concentration, especially in strain C5. Kanamycin showed the lowest antibacterial effect, with almost no inhibition at 10 and 100 mg/L and only slight activity at 1000 mg/L. Overall, ciprofloxacin was the most effective antibiotic against all tested strains (Fig. 1D; Supplementary Table 1; Supplementary file for Fig. 1).

3.5 Biochemical characteristics of isolates:

Biochemical tests (Supplementary file for Fig. 2) of all the isolated strains (C2, C4 and C5) showed positive results to methyl red test (Fig. 2A), catalase test (Fig. 2C) and oxidase test (Fig. 2G). However, citrate utilization test (Fig. 2B) and urease test (Fig. 2E) demonstrated positive reactions for C2 and C4, while negative for C5. In contrast, all isolates (C2, C4, and C5) were negative for indole test (Fig. 2D). Interestingly, strain C2 showed positive result in MSA test, while C4 and C5 were negative (Fig. 2F). However, all the strains showed negative results in the EMB test (Fig. 2H).

3.6 Identification of the bacterial isolates:

The three isolated highly arsenic-resistant bacteria (C2, C4, and C5) were identified on the basis of their similarity with other closely related bacteria whose gene sequences were obtained from the GenBank database. Such data was further used to prepare the phylogenetic trees for both isolates in order to determine the relation with other bacteria. Following 16S rRNA sequence data, the isolates C2, C4 and C5 were identified as *Bacillus sp*. (accession no. PP998418.1), *Bacillus pumilus* (accession no.

PQ061175.1), *Fictibacillus phosphorivorans* (accession no. PQ061248.1), respectively (Fig. 3; Supplementary file for Fig. 3).

3.6 Effect of different media, temperature and pH on the growth kinetics of the isolates:

All the studied arsenic resistant isolates (C2, C4, and C5) exhibited significantly ($p < 0.05$) higher growth with increasing time (0–96 h) in NB media in comparison to LB media (Fig. 4A). Similarly, in comparison to the time dependent (0–96 h) profound growth of all the isolates at pH 7, significantly ($p < 0.05$) decrease in the bacterial growth was noted at rest of the studied pH range (pH 5 and 9) (Fig. 4B). However, in case of temperature, maximum growth (within 96 h) of all the isolates was detected at 35°C temperature, whereafter their growth was found to significantly ($p < 0.05$) decline with concomitant increase in the temperature (35°C-75°C). Interestingly, despite of the high temperature, all the studied isolates were able to survive further in a wide range of pH (5–9) and temperatures (35°C-75°C) (Fig. 4C).

3.7 Minimum inhibitory concentration (MIC) under arsenic exposure:

The experimental framework was designed to evaluate bacterial tolerance to two redox forms of arsenic-sodium arsenite [As(III)] and sodium arsenate [As(V)]. Owing to the markedly higher toxicity of arsenite, each isolate was exposed to lower As(III) concentrations (5, 10, and 20 mM), whereas arsenate was applied at tenfold higher levels (50, 100, and 200 mM) to reflect its comparatively reduced toxicity. At initial concentration of arsenic, particularly arsenate form, growth of individual bacterial isolates was delayed but under consortia form their growth was triggered immediately (Fig. 5). Growth assessment of the bacterial isolate C2 was initiated at the lowest arsenite concentration (5 mM). However, further exposure resulted in a gradual decline in growth, culminating in complete growth inhibition at 200 mM arsenate, which was therefore designated as the minimum inhibitory concentration (MIC) for isolate C2 under the experimental conditions (Fig. 5). In contrast, growth assays for bacterial isolates C4 and C5 reflected similar patterns with an initial growth at 5 mM arsenite, clearly revealing a sustained and pronounced increase in growth with escalating arsenate concentrations, with maximal biomass accumulation observed at 200 mM As(V). Notably, no growth inhibition was detected even at the highest arsenate concentration tested, indicating that the MIC for isolates C4 and C5 exceeded 200 mM (Fig. 5). In either case, bacterial consortia forms exhibited duration dependent sustained enhanced growth under maximum arsenic exposure suggesting their MIC beyond 20 mM for As(III) and 200 mM for As(V).

3.9 Scanning Electron Microscopy (SEM) demonstrates morphological stability of bacteria and consortia at low arsenic levels:

SEM study of the bacterial strains (C2, C4 and C5) indicated normal morphology with intact cell wall. Similarly, their consortia (C2C4, C2C5 and C4C5) were confirmed as different forms of bacterial strains were observed to be normal and morphologically stabile under natural condition (Fig. 6; Supplementary file for Fig. 6). However, following increasing concentrations (5 and 200 mM) of arsenic exposure, signs of visible structural deformation or cell wall damage, substantial cellular aggregation and surface-associated accumulation were also found to be increased in C2 (*Bacillus sp.*), C4 (*Bacillus pumilus*) and C5 (*Fictibacillus phosphorivorans*) strains and their consortia as well when exposed to elevated arsenate concentration. Notably, minimal damaging effects on the cell wall architecture was noted in case of C4C5 consortia. Interestingly, low concentration of arsenic was unable to alter the cellular morphology in any of the studied strains (Fig. 6; Supplementary file for Fig. 6) and their consortia forms suggesting their high level of tolerance under arsenic-rich environments.

3.10 FTIR-based evidence of minimal alteration in the cell wall composition of the bacteria and consortia under low arsenic exposure:

FTIR spectral analysis of the bacterial cell wall revealed distinct structural changes in functional groups following arsenic exposure. Both in case of bacterial isolates (C2, C4 and C5) and their consortia (C2C4, C2C5 and C4C5), the broad O–H/N–H stretching band (3700 – 3200 cm^{-1}) in control samples shifted and stabilized around 3336–3339 cm^{-1} after arsenic treatment (Fig. 7; Supplementary file for Fig. 7). The aliphatic C–H stretching region (2960 – 2700 cm^{-1}) showed reduced intensity, while the triple bond region (2300 – 2150 cm^{-1}) became diminished in As treated samples when compared to the control values. The carbonyl/Amide I region shifted from 1699 – 1639 cm^{-1} in controls to approximately 1636–1638 cm^{-1} post-As-exposure in isolates and their consortia. Peaks corresponding to aromatic/NO_2 groups (1570 – 1500 cm^{-1}) and alkyl bending (1475 – 1340 cm^{-1}) decreased in intensity in As treated groups (Fig. 7; Supplementary file for Fig. 7). Bands in the 1369 – 1314 cm^{-1} range remained with slight positional changes. The C–O region (1280 – 1200 cm^{-1}) showed reduced prominence, while the fingerprint region (1162 – 1030 cm^{-1}) remained prominent. Additionally, new or intensified bands appeared in the 580 – 400 cm^{-1} region in As treated samples.

3.11 Atomic Absorption Spectroscopy (AAS)-based quantification confirmed efficient arsenic bioremediation by isolated bacterial strains and their consortia:

Quantitative estimation through AAS further confirmed the bioremediating potential of the isolate bacterial strains and their consortia. Our results revealed that all the bacterial isolates (C2, C4 and C5) exhibited profound arsenic removal efficiency (60–65%) when exposed to different arsenic concentration (5-200 ppm) (Fig. 8; Supplementary file for Fig. 8). However, in comparison to the respective bacterial strain alone, bacterial consortia (C2C4, C2C5 and C4C5) demonstrated significantly ($p < 0.05$) higher arsenic removal efficiency (78–85%) even when exposed at the highest concentration (200 ppm). Interestingly, among the studied consortia, maximum arsenic bioremediation efficiency was demonstrated by C4C5 consortia (Fig. 8; Supplementary file for Fig. 8).

4. DISCUSSION

Bioremediation of heavy metals from waste water through resistant bacterial strains is gaining attention globally due to their less implementation cost and restricted waste generation in comparison to the existing removal methods. Thus, the present study is an attempt to characterize and evaluate the utility of three arsenic resistant bacterial strains in bioremediating arsenic from wastewater. The physicochemical characterization of water samples collected from the arsenic-contaminated study site revealed significant variability across parameters, with notable associations observed between enhanced arsenic concentrations and shifts in the composition of the microbial community and their diversity. In line with the previous reports, prolonged exposure to arsenic-rich environments exerts selective pressure on indigenous microbial populations. In order to cope up the situation, highly resistant strains emerge as the are capable enough to sustain under such conditions that are usually considered to be toxic to most organisms (Tashan et al., 2021).

In the present study, three novel bacterial isolates [*Bacillus sp*. (C2), *Bacillus pumilus* (C4), *Fictibacillus phosphorivorans* (C5)] collected from arsenic-contaminated water samples in Dhapa, West Bengal, demonstrated tolerance to arsenite concentrations as high as 200 mM. Characterization and survival of these bacteria and their consortia (C2C4, C2C5 and C4C5) under such heavy arsenic exposure is the pioneer report in this area as such high concentration was found to surpass the level reported by most previously characterized arsenic-tolerant bacteria isolated from different environments (Dey et al., 2017). Such exceptional tolerance suggests not only the ecological fitness of the bacterial isolates but also underline their adaptive resistance mechanisms under arsenic mediated geochemical stress (Wu et al., 2022). On the other hand, observations regarding the biochemical studies indicated the bacteria as mesophilic as their optimal growth temperature was found to be 37°C. In addition, potentiality of all the three isolates to survive and grow at temperatures up to 75°C demonstrated their remarkable degree of thermal plasticity (Smedley et al., 2002). Similarly, wide range of tolerance across temperature and pH argues in favour of the physiological resilience of these strains. Such novel property of the strains definitely has utility in heterogeneous engineered or natural environments contaminated with heavy metals including arsenic (Sarkar et al., 2022).

In case of biochemical tests, positive reactions observed during methyl red test, catalase test and oxidase test signifies their potentiality in producing stable mixed-acid fermentation end products, capability to breakdown hydrogen peroxide due to presence of catalase enzyme activity and existence of cytochrome c oxidase enzyme activity, respectively, in all the studied bacterial strains (*Bacillus sp*., *B. pumilus* and *Fictibacillus phosphorivorans*) isolated from heavy metal contaminated wastewater (Parvathi et al., 2009; Dubey and Maheswari, 2012; Pandey et al., 2021; Golnari et al., 2024). Similarly, positive results in citrate utilization test and urease test indicated the capability of *Bacillus sp*. (C2) and *B. pumilus* (C4) to use citrate as the sole carbon source and demonstrated the potentiality of breaking down urea, respectively. However, negative reactions in both the tests signifies the inability of *Fictibacillus phosphorivorans* (C5) to utilize citrate and urea from the medium (Parvathi et al., 2009; Dubey and Maheswari, 2012; Sharma et al., 2016; Pandey et al., 2021; Golnari et al., 2024). Since, all the

isolated strains indicated negative reactions in indole test, therefore it may be argued that strain C2, C4 and C5 do not have the potentiality to produce indole from tryptophan. Similarly, differential reaction during the MSA test signifies their differential tolerance to salt rich environment. In our study, negative result in EMB test indicated the inability of all the strains (*Bacillus sp*., *B. pumilus* and *Fictibacillus phosphorivorans*) to grow in the medium which may be supported as similar responses in the same bacterial species were also reported in some earlier studies (Parvathi et al., 2009; Dubey and Maheswari, 2012; Pandey et al., 2021; Golnari et al., 2024).

Further antibiotic resistance study established their differential resistance or, susceptibility properties when exposed to diverse antibiotics. Such broad-spectrum antibiotic resistance indicated the robust adaptive mechanisms that helps these bacteria to survive in toxic metal-contaminated environments (Zhu et al., 2022). Consequently, outcome of the zone of inhibition study confirmed the sensitivity of all the wastewater derived bacterial isolates against both the forms of arsenic. In addition, differential tolerance levels of the bacterial isolates against high concentrations (≥ 200 mM) of arsenic, as depicted from the MIC study, suggested their remarkable arsenic resistance capability (Zhu et al., 2022).

Generally, arsenic resistance in bacteria has been evident to involve multiple biochemical mechanisms that helps to convert arsenic into a less toxic or transformed form with relatively reduced bioavailability potential. Such mechanisms involve enzymatic transformation through methylation-demethylation, oxidation-reduction, and precipitation reactions (Li et al., 2023). At the genetic level, *ars* operon encoding either an *arsRBC* or *arsRDABC* transcriptional array, is known to be responsible for the regulation of heavy metal resistance in bacteria. Among these, *arsB*, a membrane-associated efflux pump, is reported to reduce intracellular level of arsenite by removing it from the cytoplasm (Dey et al., 2024). Such observations clearly suggest the importance of bacterial cell wall composition in mediating the bioremediation process. In case of Gram-positive bacteria, tough and thicker cell walls serve as an additional physical barrier, restricting arsenite influx and facilitating its gene-mediated detoxification. It has also been found that in case of certain strains formation of extracellular consortium around the cell protects the intracellular organelles by reducing cytoplasmic influx of arsenic (Rojas-Solis et al., 2023). Thus, survivability and growth of the bacterial isolates in arsenic-supplemented media, as observed in our viable cell count assay, clearly suggested their capability in utilizing arsenic as a supplementary energy source (Hassan et al., 2022). Such assumptions earn support as different bacterial strains have been found to possess particular sets of genes (*aoxR*, *aoxB*, and *aoxC*) as part of the arsenite oxidase system responsible for oxidizing arsenic in environment (Chang et al., 2010; Li et al., 2023). Moreover, it is well accepted that heterotrophic arsenite-oxidizing bacteria implies this oxidation as a detoxification mechanism, while autotrophic individuals directly use arsenite as an electron donor for energy generation (Mandal et al., 2022). Therefore, it may be argued that the bacterial strains isolated from the wastewater and their consortia might have oxidized arsenite as an usual metabolic response and detoxification repertoire as reported in other studies also (Mandal et al., 2022; Kumar et al., 2022).

In order to understand the remediation mechanism of the bacterial strains, SEM study was conducted to investigate any possible effect of arsenic on their cell wall architecture. Since, the overall cellular

architecture of the cell was not severely disrupted, it may be argued that the strains possess effective protective or adaptive mechanisms that allow it to withstand elevated arsenic concentrations without undergoing complete cellular breakdown. This resilience indicates that the bacterium possesses protective mechanisms that enable survival and stability even under elevated arsenic stress (Malik et al., 2022; Li et al., 2023); however, the exact mechanism remained unexplored. In our study, exposure to high arsenic concentrations (≥ 200 mM) triggered profound strain-specific stress responses reflecting considerable functional heterogeneity within the microbial community (Kumar et al., 2022). Ultrastructural microscopic studies revealed that strains C2 and C5 exhibited detectable arsenic-induced cellular stress as severe membrane and cell wall damage was noted. Such observations confirmed a relatively lesser tolerance of the strains to arsenic toxicity. However, no major disruption in the cell wall architecture in C5 and the studied consortia indicated the presence of robust protective and adaptive mechanisms. Despite of some damaging notions in the cell wall of the consortia, majority of the population was found to be structurally stable and metabolically active under extreme arsenic stress. Among the different studied consortia, C4C5 revealed minimal modifications in the outer cell wall architecture indicating localized envelope damage rather than extensive cellular damage (Flores et al., 2022). These findings collectively emphasize on the role of microbial synergist, functional redundancy, and endogenous detoxification mechanisms in maintaining community-level resilience in diverse environments contaminated with relatively higher levels of heavy metal (Yang et al., 2012; Uddin et al., 2021).

FTIR analysis added further mechanistic insights into the interaction between bacterial cell wall composition and different arsenic species. In untreated control samples of C2, C4, and C5, a broad O-H/N-H stretching band spanning 3700 – 3200 cm^{-1} indicated an extensive hydrogen-bonded network on the cell surface (Matten et al., 2020). Following exposure to both low-concentration As(III) and high-concentration As(V), this band sharpened and stabilized at approximately 3336–3339 cm^{-1}, indicative of hydrogen bond reorganization and direct participation of hydroxyl and amino groups in arsenic coordination (Dube et al., 2023). A marked reduction in the aliphatic C-H stretching region (2960 – 2700 cm^{-1}) after arsenic treatment suggested partial masking or involvement of alkyl chains during surface complexation, while the disappearance of bands in the triple bond region (2300 – 2150 cm^{-1}) indicated that nitrile or alkyne functional groups do not contribute significantly to arsenic binding. A consistent downfield shift in the carbonyl/Amide I region from 1699 – 1639 cm^{-1} in controls to approximately 1636–1638 cm^{-1} in treated samples reflected electronic perturbation of conjugated carbonyl and amide functionalities attributable to arsenic coordination. Reduced intensities in the aromatic/NO_2 (1570 – 1500 cm^{-1}) and alkyl bending (1475 – 1340 cm^{-1}) regions suggested only minor structural rearrangements at these sites, while persistent bands corresponding to C-N and phenolic O-H vibrations (1369 – 1314 cm^{-1}) supported their active role in metal binding. The fingerprint region (1162 – 1030 cm^{-1}), associated with C-O and C-O-C vibrations of ether and alcohol functionalities, remained prominent across all treated samples, identifying these moieties as principal adsorption sites. Most critically, the emergence and intensification of bands within the 580 – 400 cm^{-1} region in arsenic-treated samples

provided definitive spectroscopic evidence of As-O bond formation, confirming successful arsenic complexation at the cell surface (William et al., 2023). Collectively, these spectral shifts demonstrate that hydroxyl, amino, carbonyl, and ether groups collectively mediate arsenic adsorption through modification of pre-existing surface functional groups rather than structural degradation of the cell (Dube et al., 2023).

In light of the gathered evidences, it was essential to further quantify the bioremediation efficacy of the bacterial isolates and their consortia; thus, AAS study was conducted. Our study demonstrated that the arsenic resistant bacterial isolates individually can achieve approximately 60% removal of arsenate and 50% removal of arsenite from nutrient broth amended with the respective arsenic species within 96 hours. Notably, the consortia formed from pairwise combinations - C2C4, C2C5, and C4C5 - exhibited removal efficiencies exceeding 60% for both arsenate and arsenite, indicating a synergistic enhancement of bioremediation capacity in co-culture conditions. The observed bacteria mediated decrease in arsenic level might be a resultant of the biotransformation and bioprecipitation processes regulated by specific resistance and detoxification genes (Sarkar et al., 2022). Such an enhancement in the bioremediation potential can be attributed to the synergistic metabolic and adsorption capabilities of multiple bacterial species working together; thus, achieving improved metal bioaccumulation and transformation (Sarkar et al., 2022). Based on the finding of the present study, field application will be necessary to test the superior potential of bacterial consortia for large-scale bioremediation applications in environments contaminated with multi-heavy metals (Kruger et al., 2013). Moreover, utilization of the microbial oxidation of arsenite to arsenate, as demonstrated by these isolates, may be beneficial for water treatment applications as no conventional chemical oxidation approaches are required (William et al., 2023).

5. CONCLUSION

To the best of our knowledge, this study represents the first report of naturally occurring arsenic-resistant bacteria in the arsenic-contaminated water bodies of Dhapa, West Bengal, exhibiting the combined capacity for arsenic removal, biotransformation, and oxidation as integrated components of their metabolic and detoxification machinery. Our study demonstrates the successful isolation, characterization, and molecular identification of arsenic-resistant bacterial strains with significant potential for bioremediation of contaminated environments. The isolates exhibited remarkable arsenic tolerance and removal efficiency, exceeding 60% under controlled conditions. Their ability to withstand high concentrations of both arsenite and arsenate highlights robust adaptive mechanisms that enable survival under extreme metal stress. Antibiotic resistance patterns further suggest resilience and environmental competitiveness, while FTIR and SEM analyses revealed metabolic and structural adaptations linked to detoxification processes and cellular protection.

It has been further speculated that mechanistically, these bacteria employ a multifaceted resistance network involving arsenic uptake, enzymatic transformation, active efflux, and possible metabolic utilization. The interplay of arsenate reduction, arsenite oxidation, and transport systems may have

underscored a highly coordinated detoxification strategy; however, the exact mechanism remained unexplored and requires further investigation. Additionally, biosorption via functional groups on cell surfaces and the formation of microbial consortia enhance arsenic immobilization and removal efficiency. Thus, it may be argued that these novel strains represent promising candidates for deployment in arsenic bioremediation strategies targeting contaminated drinking water sources. Overall, these findings reinforce the ecological and biotechnological relevance of arsenic-resistant bacteria as sustainable, cost-effective alternatives to conventional remediation methods. Future investigations into genetic determinants and field-scale applications will be critical for translating these insights into practical environmental and agricultural solutions.

Declarations

Acknowledgements:

The authors thankfully acknowledge Department of Biotechnology and Microbiology, Swami Vivekananda University, Kolkata, India for providing the necessary facilities. FESEM facility of Visva-Bharati is also thankfully acknowledged.

Credit Authorship Contribution Statement:

Arpita Chakraborty: Writing-original draft, Writing-review & editing, Data curation, Investigation, Resources, Formal analysis, Methodology, Software, Visualization.

Samudra Pal: Software, Formal analysis, Preparation of figure, Writing-review & editing

Tuhin Mukherjee: Investigation, Methodology, Writing-review & editing

Tanya Das: Investigation, Methodology, Writing-review & editing

Nimai Chandra Saha: Writing - review & editing, Validation, Formal analysis

Palash Kumar Pal: Conceptualization, Funding acquisition, Project administration, Supervision, Writing-review & editing, Resources, Validation, Formal analysis, Methodology, Software, Visualization

Declaration of Competing Interest:

The authors declare that they have no known financial or personal conflicts of interest that could have influenced the work presented in this paper.

Funding Sources: No specific fund was available.

Data Availability: The data supporting the present study's findings can be obtained from the corresponding author upon reasonable request.

References

1. Adetunji AI, Oberholster PJ, Erasmus M (2023) Bioleaching of metals from e-waste using microorganisms: a review. Minerals 13(6):828. https://doi.org/10.3390/min13060828
2. Aliyari Rad S, Nobaharan K, Pashapoor N, Pandey J, Dehghanian Z, Senapathi V, Asgari Lajayer B (2023) Nano-microbial remediation of polluted soil: a brief insight. Sustainability 15(1):876. https://doi.org/10.3390/su15010876
3. Aluko OA, Opoku EEO, Ibrahim M (2021) Investigating the environmental effect of globalization: insights from selected industrialized countries. J Environ Manage 281:111892. https://doi.org/10.1016/j.jenvman.2020.111892
4. Alves AR, Yin Q, Oliveira RS, Silva EF, Novo LA (2022) Plant growth-promoting bacteria in phytoremediation of metal-polluted soils: current knowledge and future directions. Sci Total Environ 838:156435. https://doi.org/10.1016/j.scitotenv.2022.156435
5. Arce-Inga M, González-Pérez AR, Hernandez-Diaz E, Chuquibala-Checan B, Chavez-Jalk A, Llanos-Gomez KJ, Cumpa-Velasquez LM (2022) Bioremediation potential of native Bacillus sp. strains as a sustainable strategy for cadmium accumulation of *Theobroma cacao* in Amazonas region. Microorganisms 10(11):2108. https://doi.org/10.3390/microorganisms10112108
6. Ayangbenro AS, Babalola OO, Aremu OS (2019) Bioflocculant production and heavy metal sorption by metal resistant bacterial isolates from gold mining soil. Chemosphere 231:113–120. https://doi.org/10.1016/j.chemosphere.2019.05.092
7. Bertin PN, Crognale S, Plewniak F, Battaglia-Brunet F, Rossetti S, Mench M (2022) Water and soil contaminated by arsenic: the use of microorganisms and plants in bioremediation. Environ Sci Pollut Res 29(7):9462–9489. https://doi.org/10.1007/s11356-021-17817-4
8. Bhatt P, Chaudhary P, Ahmad S, Bhatt K, Chandra D, Chen S (2023) Recent advances in the application of microbial inoculants in the phytoremediation of xenobiotic compounds. In: Unravelling plant-microbe synergy, pp 37–48. https://doi.org/10.1016/B978-0-323-99896-3.00013-8
9. Bukhari DA, Rehman A (2023) Metal-resistant bacteria as a green bioresource for arsenic remediation in wastewaters. Curr Opin Green Sustainable Chem 40:100785. https://doi.org/10.1016/j.cogsc.2023.100785
10. Cao X, Cui X, Xie M, Zhao R, Xu L, Ni S, Cui Z (2022) Amendments and bioaugmentation enhanced phytoremediation and micro-ecology for PAHs and heavy metals co-contaminated soils. J Hazard Mater 426:128096. https://doi.org/10.1016/j.jhazmat.2021.128096
11. Chang JS, Kim HJ, Lee JH (2024) Detoxification of ars genotypes by arsenite-oxidizing bacteria through arsenic biotransformation. Environ Geochem Health 46(11):470. https://doi.org/10.1007/s10653-024-02251-5
12. Darma A, Yang J, Bloem E, Możdżen K, Zandi P (2022) Arsenic biotransformation and mobilization: the role of bacterial strains and other environmental variables. Environ Sci Pollut Res 29(2):1763–1787. https://doi.org/10.1007/s11356-021-17117-x

13. Das A, Bandopadhyay DK, Jee PK, Karmakar A (2014) Geochemistry of sediments and water with a health risk assessment of heavy metal contaminated vegetables grown in Dhapa, a waste disposal site in Kolkata, India. World Rev Sci Technol Sustainable Dev 11(3–4):248–268. https://doi.org/10.1504/WRSTSD.2014.066817
14. Dey U et al (2017) Bioremediation of arsenic. Environ Processes 4(1):183–199. https://doi.org/10.1007/s40710-017-0219-7
15. Dey U, Mondal NK, Chatterjee S, Das K, Raj D, Kumar P, Meraj G (2024) Isolation and identification of novel arsenic-resistant bacteria from an arsenic-contaminated region-a study to understand the efficiency of bacteria for arsenic removal from aqueous media. Water 16(17):2401. https://doi.org/10.3390/w16172401
16. Doane M, Haggerty JM, da Silva Lopes CR, Yates P, Edwards R, Dinsdale E, Bruce T (2020) Latitude and chlorophyll a density drive the distribution of carbohydrate-active enzymes in the planktonic microbial fraction of the epipelagic zone. Environ Microbiol Rep 12(5):473–485. https://doi.org/10.1111/1758-2229.12865
17. Dube R, Singh S, Gupte A, Modi A (2023) Arsenic contamination in Bihar, India: exploring the impact, mitigation, and bioremediation strategies. https://doi.org/10.21203/rs.3.rs-3286620/v1
18. Dubey RC, Maheswari DK (2012) Practical microbiology 4/e. R.C. Dubey and D.K. Maheshwari (Eds.) Edition 3. Publisher: S Chand & Company, P Ltd, New Delhi, India
19. Fadlelmoula A, Pinho D, Carvalho VH, Catarino SO, Minas G (2022) Fourier transform infrared (FTIR) spectroscopy to analyse human blood over the last 20 years: a review towards lab-on-a-chip devices. Micromachines 13(2):187. https://doi.org/10.3390/mi13020187
20. Faghihzadeh F, Anaya NM, Schifman LA, Oyanedel-Craver V (2016) Fourier transform infrared spectroscopy to assess molecular-level changes in microorganisms exposed to nanoparticles. Nanatechnol Environ Eng 1(1):1. https://doi.org/10.1007/s41204-016-0001-8
21. Flores A, Valencia-Marín MF, Chávez-Avila S, Ramírez-Díaz MI, de Los Santos-Villalobos S, Meza-Carmen V, Santoyo G (2022) Genome mining, phylogenetic, and functional analysis of arsenic (As) resistance operons in *Bacillus* strains isolated from As-rich hot spring microbial mats. Microbiol Res 264:127158. https://doi.org/10.1016/j.micres.2022.127158
22. Ghosh R, Hazra T, Mukherjee I, Ushcats S, Wasim Akram M, Akram MA, Vlasenko O (2024) Evaluating the environmental effects of open dumps and waste farming: a case study of open dumping. Ecol Questions 35(4):39–51. https://doi.org/10.1128/JB.00128-19
23. Golnari M, Bahrami N, Milanian Z, Rabbani Khorasgani M, Asadollahi MA, Shafiei R, Fatemi SSA (2024) Isolation and characterization of novel *Bacillus* strains with superior probiotic potential: comparative analysis and safety evaluation. Sci Rep 14(1):1457. 10.1038/s41598-024-51823-z
24. Hassan A, Pariatamby A, Ossai IC, Ahmed A, Muda MA, Wen TZ, Hamid FS (2022) Bioaugmentation-assisted bioremediation and kinetics modelling of heavy metal-polluted landfill soil. Int J Environ Sci Technol 19(7):6729–6754. https://doi.org/10.1007/s13762-021-03626-2

25. He C, Liu N, Li F, Jia X, Peng H, Liu Y, Xiao Y (2019) Complex structure of Pseudomonas aeruginosa arginine rhamnosyltransferase EarP with its acceptor elongation factor P. J Bacteriol 201(13):e00128–e00119. https://doi.org/10.1128/JB.00128-19
26. Kaparwan D, Rana NS, Dhyani BP (2020) Heavy metals toxicity in agricultural soils: critical review of possible sources, influence on soil health and remedial measures to remove, reduce and stabilize contaminants. Int J Curr Microbiol Appl Sci 9(6):1467–1482. https://doi.org/10.20546/ijcmas.2020.906.182
27. Kasprowicz MJ, Kozioł M, Gorczyca A (2010) The effect of silver nanoparticles on phytopathogenic spores of *Fusarium culmorum*. Can J Microbiol 56(3):247–253. https://doi.org/10.1139/w10-012
28. Kepenek ES, Gozen AG, Severcan F (2019) Molecular characterization of acutely and gradually heavy metal acclimated aquatic bacteria by FTIR spectroscopy. J Biophotonics 12(5):e201800301. https://doi.org/10.1002/jbio.201800301
29. Khandelwal R, Keelka S, Jain N, Jain P, Kumar Sharma M, Kaushik P (2024) Biosorption of arsenic (III) from aqueous solution using calcium alginate immobilized dead biomass of Acinetobacter sp. strain Sp2b. Sci Rep 14(1):9972. https://doi.org/10.1038/s41598-024-60329-7
30. Kruger MC, Bertin PN, Heipieper HJ, Arsène-Ploetze F (2013) Bacterial metabolism of environmental arsenic-mechanisms and biotechnological applications. Appl Microbiol Biotechnol 97(9):3827–3841. https://doi.org/10.1007/s00253-013-4838-5
31. Kumar V, Singh G, Dwivedi SK (2022) Arsenic and nickel stress response, their bioremediation potential and mechanism of *Trichoderma lixii* isolated from electroplating wastewater. Geomicrobiol J 39(3–5):186–198. https://doi.org/10.1080/01490451.2021.1956648
32. Li Y, Guo L, Yang R, Yang Z, Zhang H, Li Q, Sun W (2023) *Thiobacillus* spp. and *Anaeromyxobacter* spp. mediate arsenite oxidation-dependent biological nitrogen fixation in two contrasting types of arsenic-contaminated soils. Journal of Hazardous Materials 443:130220. https://doi.org/10.1016/j.jhazmat.2022.130220
33. Lin Y, Zhang H, Li P, Jin J, Li Z (2022) The bacterial consortia promote plant growth and secondary metabolite accumulation in *Astragalus mongholicus* under drought stress. BMC Plant Biol 22(1):475. https://doi.org/10.1186/s12870-022-03859-4
34. Malik S, Kishore S, Shah MP, Kumar SA (2022) A comprehensive review on nanobiotechnology for bioremediation of heavy metals from wastewater. J Basic Microbiol 62(3–4):361–375. https://doi.org/10.1002/jobm.202100555
35. Mandal D, Sonar R, Saha I, Ahmed S, Basu A (2022) Isolation and identification of arsenic resistant bacteria: a tool for bioremediation of arsenic toxicity. Int J Environ Sci Technol 19(10):9883–9900. https://doi.org/10.1007/s13762-021-03673-9
36. Merino LE, Llana MN, Garófalo A, Trejo FM, Golowczyc MA (2025) Antibiofilm properties of lactic acid bacteria and their metabolites against *Salmonella enterica* serotype Enteritidis on eggshell surface. Curr Res Microb Sci 8:100384. https://doi.org/10.1016/j.crmicr.2025.100384

37. Matten KJ, Parrott JL, Bartlett AJ, Gillis PL, Milani D, Toito J, Prosser RS (2020) Toxicity of dinonylnaphthalene sulfonates to *Pimephales promelas* and epibenthic invertebrates. Sci Total Environ 741:140260. https://doi.org/10.1016/j.scitotenv.2020.140260
38. Mohamed MS, Hozayen WG, Alharbi RM, Ibraheem IBM (2022) Adsorptive recovery of arsenic (III) ions from aqueous solutions using dried *Chlamydomonas* sp. Heliyon 8(12):e12398. https://doi.org/10.1016/j.heliyon.2022.e12398
39. Naiel MA, Taher ES, Rashed F, Ghazanfar S, Shehata AM, Mohammed NA, Shukry M (2024) Arsenic bioremediation using genetically engineered microbial strains in aquatic environments: an updated overview. Heliyon 10(17):e36314. https://doi.org/10.1016/j.heliyon.2024.e36314
40. Pandey N, Bhatt R (2015) Arsenic resistance and accumulation by two bacteria isolated from a natural arsenic contaminated site. J Basic Microbiol 55(11):1275–1286. https://doi.org/10.1002/jobm.201400723
41. Pandey R, Sharma P, Rathee S, Singh HP, Batish DR, Krishnamurthy B, Kohli RK (2021) Isolation and characterization of a novel hydrocarbonoclastic and biosurfactant producing bacterial strain: *Fictibacillus phosphorivorans* RP3. 3 Biotech 11(2):105. 10.1007/s13205-021-02655-5
42. Parvathi A, Krishna K, Jose J, Joseph N, Nair S (2009) Biochemical and molecular characterization of *Bacillus pumilus* isolated from coastal environment in Cochin, India. Brazilian J Microbiol 40(2):269–275. 10.1590/S1517-838220090002000012
43. Praveen R, Nagalakshmi R (2022) Review on bioremediation and phytoremediation techniques of heavy metals in contaminated soil from dump site. Materials Today: Proceedings 68:1562–1567. https://doi.org/10.1016/j.matpr.2022.07.190
44. Preetha JSY, Arun M, Vidya N, Kowsalya K, Halka J, Ondrasek G (2023) Biotechnology advances in bioremediation of arsenic: a review. Molecules 28(3):1474. https://doi.org/10.3390/molecules28031474
45. Rojas-Solis D, Larsen J, Lindig-Cisneros R (2023) Arsenic and mercury tolerant rhizobacteria that can improve phytoremediation of heavy metal contaminated soils. PeerJ 11:e14697. https://doi.org/10.7717/peerj.14697
46. Roy T, Das N (2017) Isolation, characterization, and identification of two methomyl-degrading bacteria from a pesticide-treated crop field in West Bengal, India. Microbiology 86(6):753–764. https://doi.org/10.1134/S0026261717060145
47. Sarkar A, Paul B, Darbha GK (2022) Groundwater arsenic contamination in the Bengal Basin: a brief review. Chemosphere 299:134369. https://doi.org/10.1016/j.chemosphere.2022.134369
48. Shah N, Dubey VK, Thakkar S, Doshi H, Mahawar P (2022) Bioaccumulation of arsenic (V) from wastewater by live and dead Spirogyra sp. J Basic Microbiol 62(3–4):489–497
49. Sharma A, Kohli P, Singh Y, Schumann P, Lal R (2016) *Fictibacillus halophilus* sp. nov., from a microbial mat of a hot spring atop the Himalayan Range. Int J Syst Evol MicroBiol 66(6):2409–2416. 10.1099/ijsem.0.001051

50. Sher S, Ishaq MT, Bukhari DA, Rehman A (2023) Brevibacterium sp. strain CS2: a potential candidate for arsenic bioremediation from industrial wastewater. Saudi J Biol Sci 30(10):103781. https://doi.org/10.1016/j.sjbs.2023.103781
51. Tashan H, Harighi B, Rostamzadeh J, Azizi A (2021) Characterization of arsenic-resistant endophytic bacteria from alfalfa and chickpea plants. Front Plant Sci 12:696750. https://doi.org/10.3389/fpls.2021.696750
52. Uddin MJ, Ampiaw RE, Lee W (2021) Adsorptive removal of dyes from wastewater using a metal-organic framework: a review. Chemosphere 284:131314. https://doi.org/10.1016/j.chemosphere.2021.131314
53. Wang P, Du H, Fu Y, Cai X, Yin N, Cui Y (2022) Role of human gut bacteria in arsenic biosorption and biotransformation. Environ Int 165:107314. https://doi.org/10.1016/j.envint.2022.107314
54. William VU, Magpantay HD (2023) Arsenic and microorganisms: genes, molecular mechanisms, and recent advances in microbial arsenic bioremediation. Microorganisms 12(1):74. https://doi.org/10.3390/microorganisms12010074
55. Wu P, Zhang Z, Luo Y, Bai Y, Fan J (2022) Bioremediation of phenolic pollutants by algae: current status and challenges. Bioresour Technol 350:126930. https://doi.org/10.1016/j.biortech.2022.126930
56. Yang HC, Fu HL, Lin YF, Rosen BP (2012) Pathways of arsenic uptake and efflux. In: Current topics in membranes, vol 69, pp 325–358. Academic Press. https://doi.org/10.1016/B978-0-12-394390-3.00012-4
57. Zeng G, He Y, Liang D, Wang F, Luo Y, Yang H, Sun D (2022) Adsorption of heavy metal ions copper, cadmium and nickel by Microcystis aeruginosa. Int J Environ Res Public Health 19(21):13867. https://doi.org/10.3390/ijerph192113867
58. Zhu X, Li X, Shen B, Zhang Z, Wang J, Shang X (2022) Bioremediation of lead-contaminated soil by inorganic phosphate-solubilizing bacteria immobilized on biochar. Ecotoxicol Environ Saf 237:113524. https://doi.org/10.1016/j.ecoenv.2022.113524

Tables

Table 1: Estimated concentrations of different heavy metals in the wastewater

Sl. No.	Test parameter	Test Method	Concentration (ppm)
1	Cadmium (Cd)	IS 3025: PART 41: 2023	< 0.02
2	Total Chromium (Cr)	IS 3025: PART 52: 1994	0.31
3	Lead (Pb)	IS 3025: PART 47: 1994	0.26
4	Total Arsenic (As)	IS 3025: PART 37: 2022	< 0.10

Figures

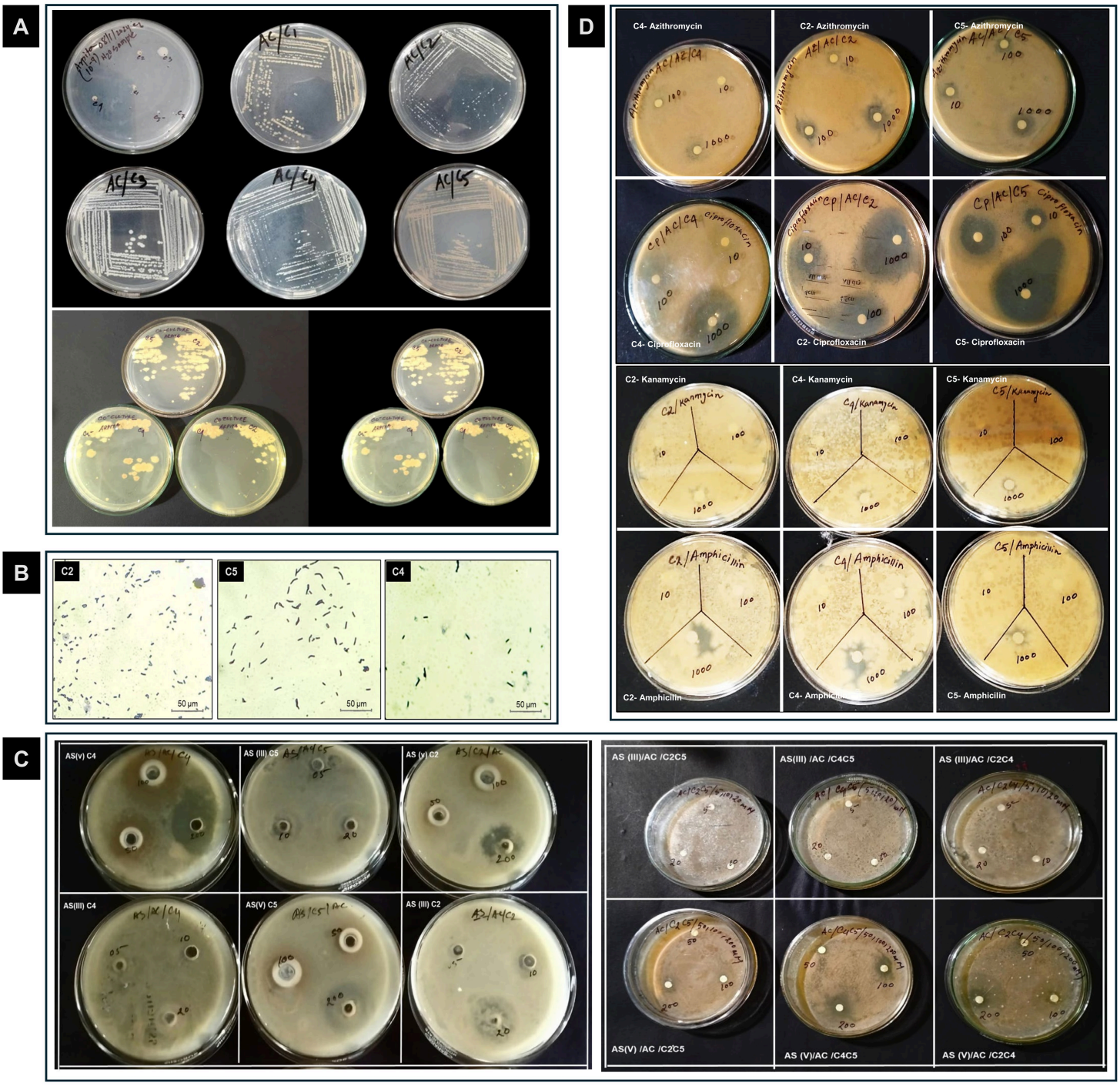


Figure 1

Representative images showing the observations of the different morphological and biochemical characterization tests of the bacterial strains (C2, C4 and C5) isolated from heavy metal contaminated wastewater and their consortia. **(A)**isolation of arsenic resistant bacteria and their morphological characteristics, **(B)** gram-staining, **(C)** zone of inhibition, and **(D)**antibiotic test.

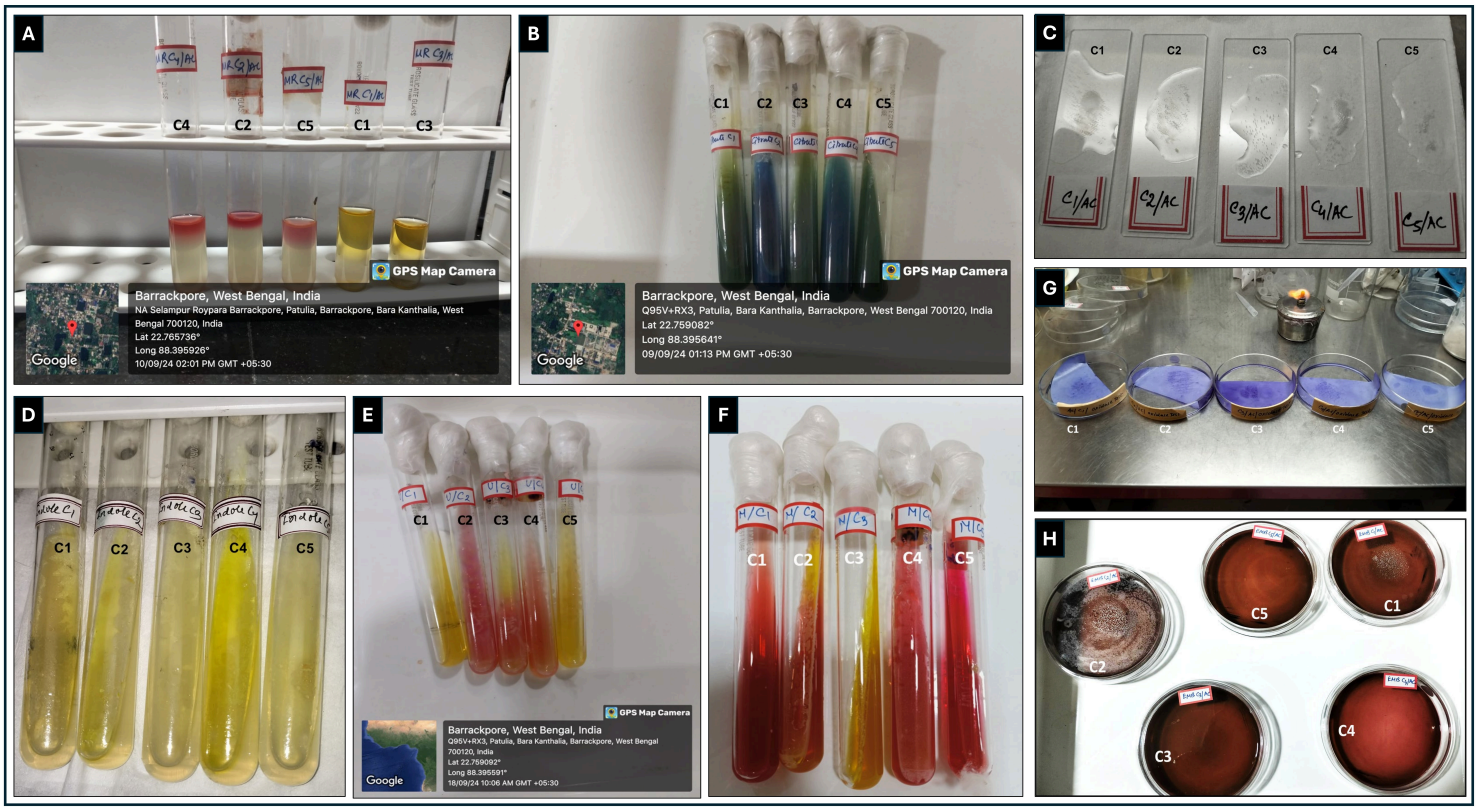


Figure 2

Representative images showing the observations of the different biochemical characterization tests of the bacterial strains (C2, C4 and C5) isolated from heavy metal contaminated wastewater and their consortia. **(A)** Methyl red test, **(B)** citrate test, **(C)** catalase test, and **(D)** indole test, **(E)** urease test, **(F)** MSA test, **(G)** oxidase test, and **(H)**EMB test.

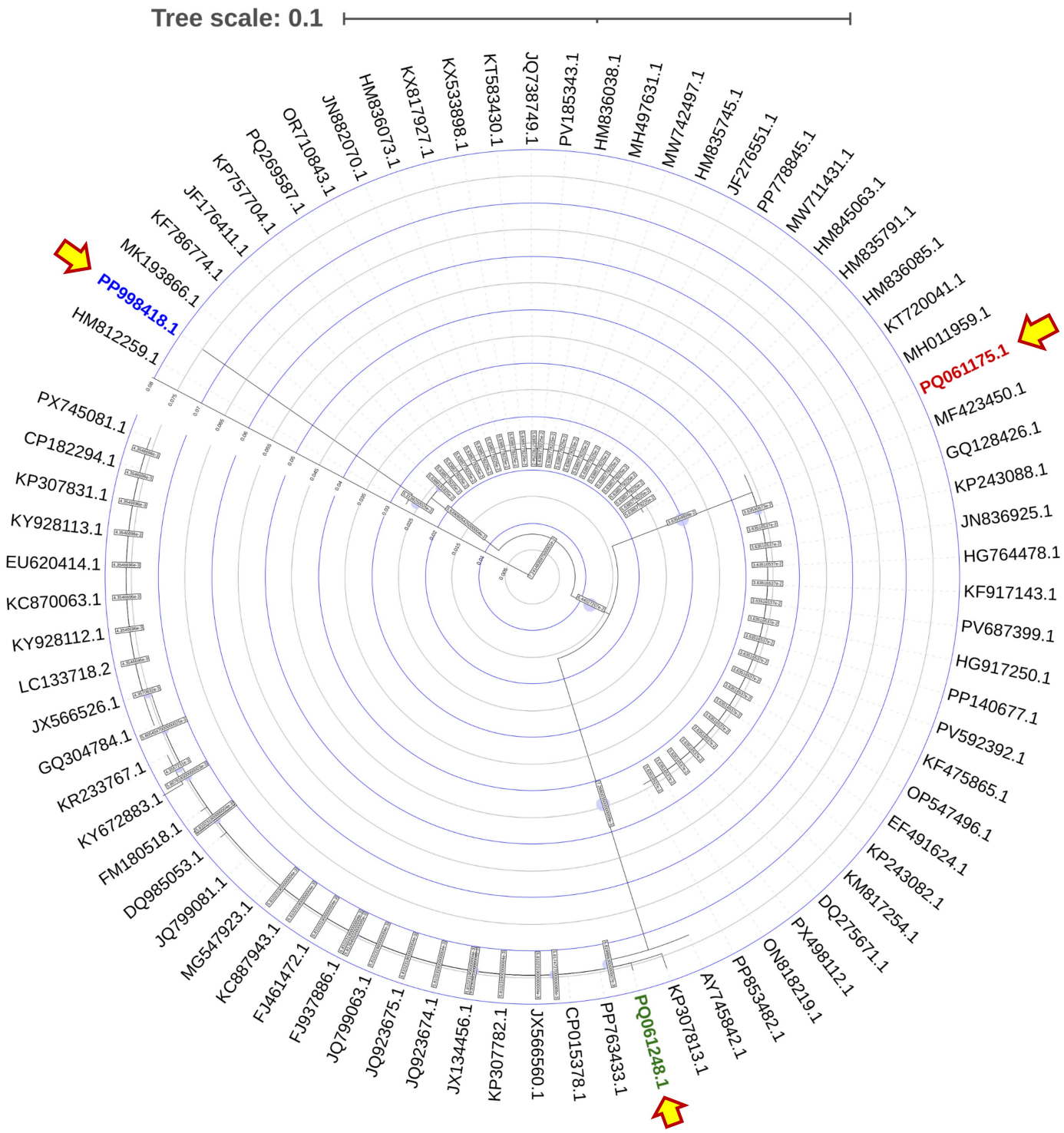


Figure 3

Phylogenetic tree representing identity of the bacterial isolates following 16S rRNA sequence data where the isolates C2, C4 and C5 were identified as *Bacillus* sp. (accession no. PP998418.1), *Bacillus pumilus* (accession no. PQ061175.1), *Fictibacillus phosphorivorans*(accession no. PQ061248.1), respectively.

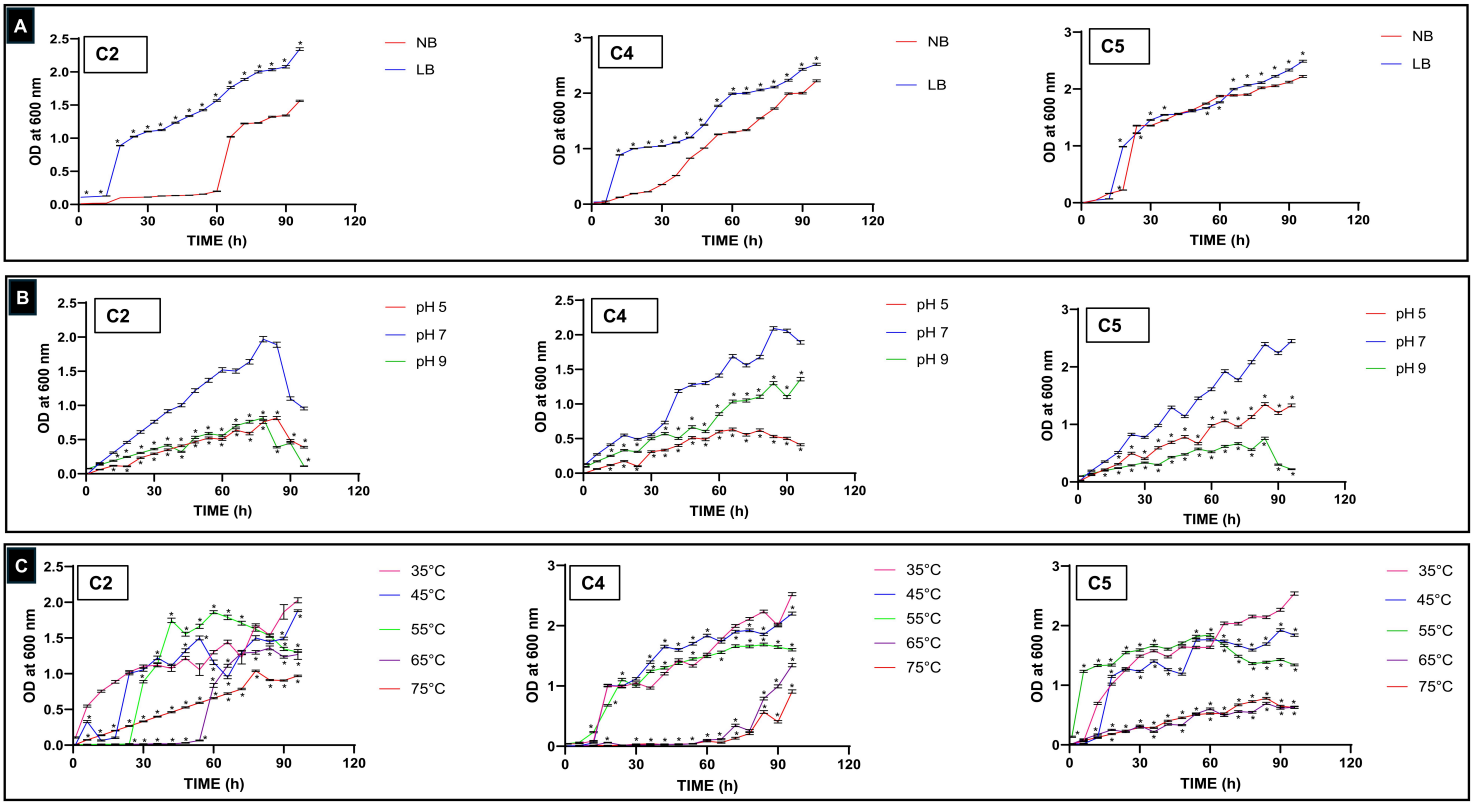


Figure 4

Graphical representation of the data (Mean ± SEM) on effects of different media (NB and LB), pH and temperature for growth optimization of the bacterial strains (C2, C4 and C5) isolated from heavy metal contaminated wastewater. **(A)** Asterix (*) indicated significant (p<0.05) change in the bacterial growth in LB media at a particular time point compared to the values in NB group following one-way ANOVA. **(B)** Asterix (*) indicated significant (p<0.05; vs. pH 7) change in the bacterial growth at a particular time point under a specific pH (either pH 5 or, pH 9) following one-way ANOVA. **(C)** Asterix (*) indicated significant (p<0.05; vs. 35°C) change in the bacterial growth at a particular time point under a specific temperature (45°C or, 55°C or, 65°C or, 75°C) following one-way ANOVA.

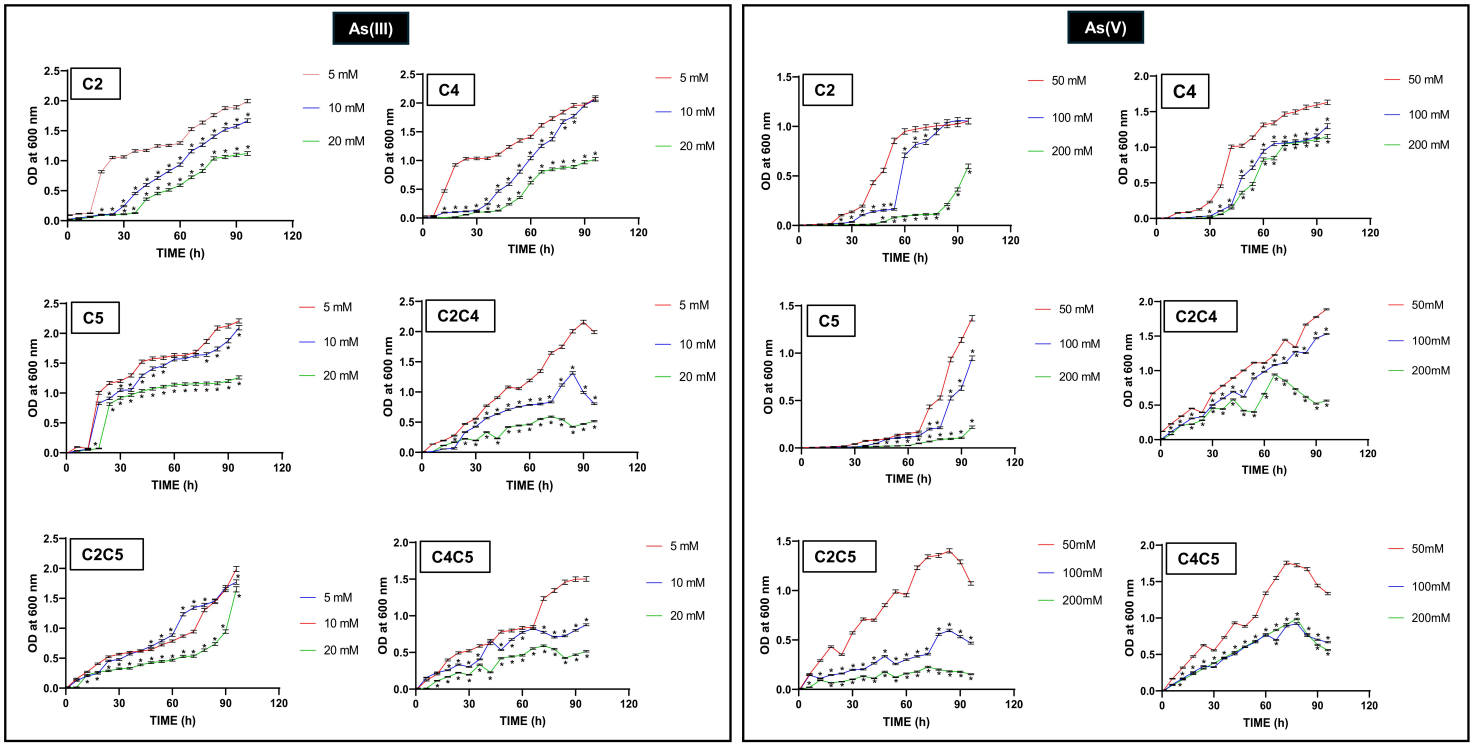


Figure 5

Graphical representation of the minimum inhibitory concentration (MIC) under arsenic exposure in bacterial strains (C2, C4 and C5) isolated from heavy metal contaminated wastewater and their consortia (C2C4, C2C5 and C4C5). The bacterial isolates individually and their consortia forms were subjected to two redox forms of arsenic- sodium arsenite [As(III)] and sodium arsenate [As(V)]. As(III) was tested at concentrations (5, 10, and 20 mM), whereas As(V) was applied at tenfold higher levels (50, 100, and 200 mM) to reflect its comparatively reduced toxicity. Growth of bacterial strains alone or in consortia states were recorded for 96 h. In either case, bacterial consortia forms exhibited duration dependent sustained enhanced growth under maximum arsenic exposure suggesting their MIC beyond 20 mM for As(III) and 200 mM for As(V). In case of As(III), asterix (*) indicated significant (p<0.05; vs. 5 mM) change in the bacterial growth at a particular time point under a specific arsenic exposure (either 10 mM or, 20 mM) following one-way ANOVA. While, in case of As(V), asterix (*) indicated significant (p<0.05; vs. 50 mM) change in the bacterial growth at a particular time point under a specific arsenic exposure (either 100 mM or, 200 mM) following one-way ANOVA.

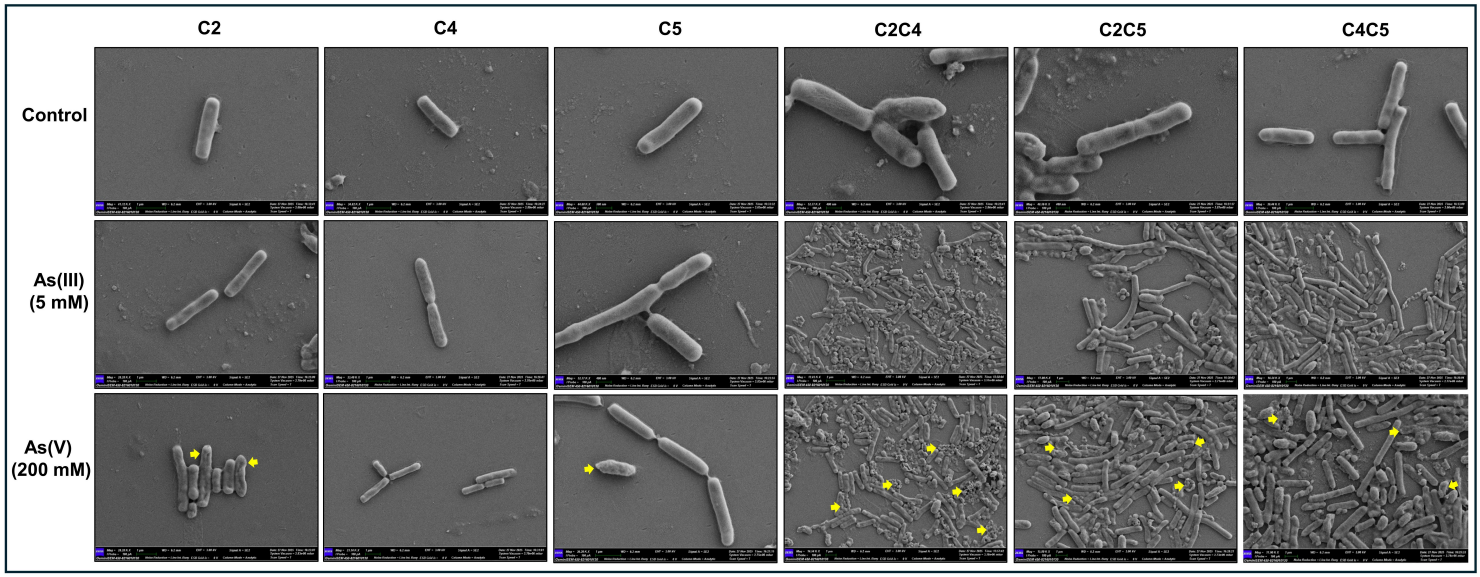


Figure 6

Representative images of Scanning Electron Microscopy (SEM) of the bacterial isolates (C2, C4 and C5) and their consortia (C2C4, C2C5 and C4C5) demonstrating morphological stability of bacteria and consortia at low and high arsenic concentrations. In untreated control samples, normal and morphologically stable cell wall is observed. However, following increasing concentrations (5-200 mM) of arsenic exposure, signs of visible structural deformation or cell wall damage (marked as yellow arrows) were found to increase along with enhanced substantial cellular aggregation and surface-associated accumulation. High arsenic exposure was found to cause minimal damaging effects on the cell wall architecture of C4C5 consortia. However, low concentration of arsenic was unable to alter the cellular morphology in any of the studied strains and their consortia forms suggesting their high level of tolerance under arsenic-rich environments.

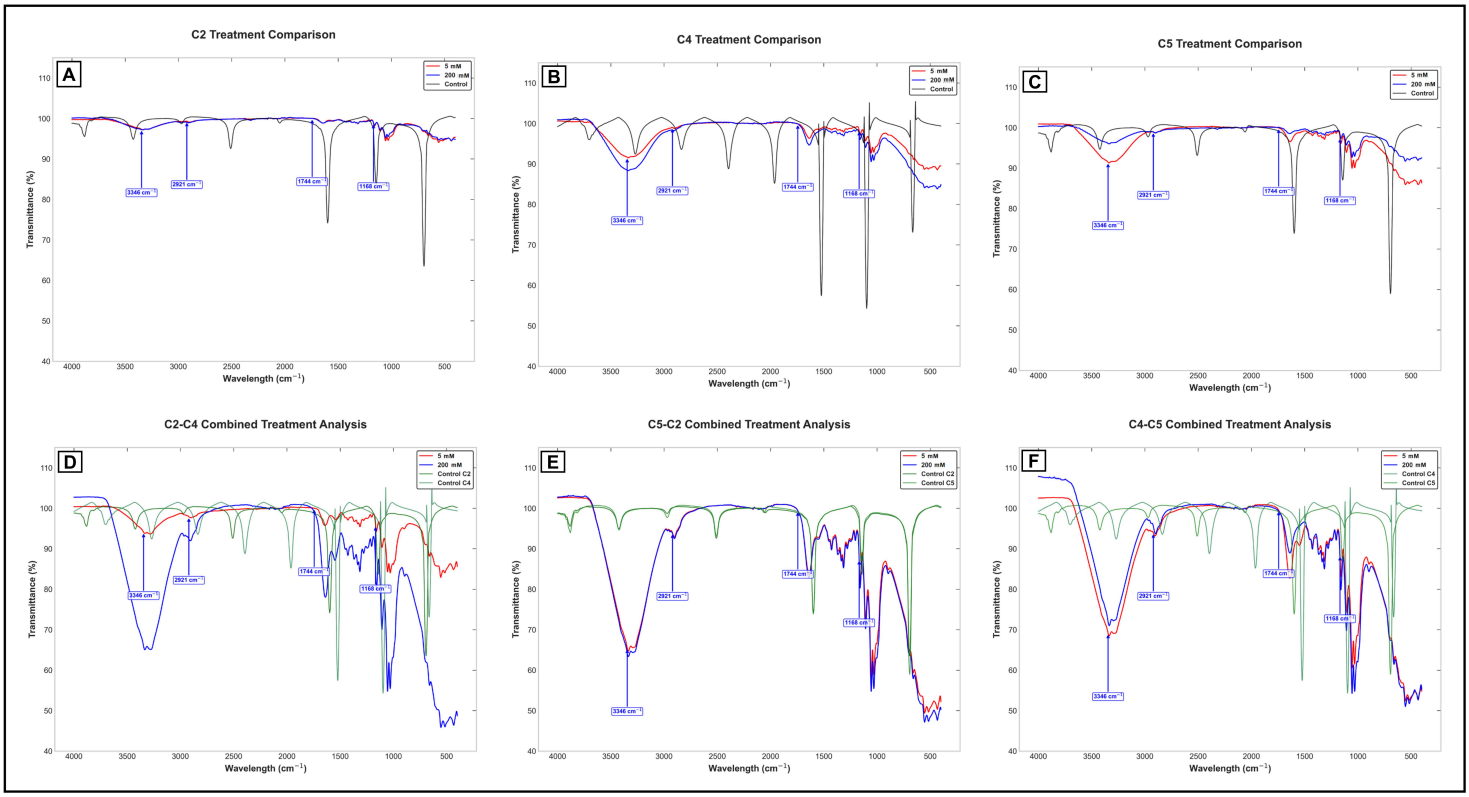


Figure 7

FTIR-based evidences of minimal alteration in the cell wall composition of the **(A-C)** isolated bacteria and **(D-F)** their consortia under low arsenic exposure. In untreated control samples of bacterial isolates (C2, C4 and C5) and their consortia (C2C4, C2C5 and C4C5), the broad O-H/N-H stretching band (3700-3200 cm^{-1}) in control samples shifted and stabilized around 3336-3339 cm^{-1} after arsenic treatment indicating hydrogen bond reorganization and direct participation of hydroxyl and amino groups in arsenic coordination. The aliphatic C-H stretching region (2960-2700 cm^{-1}) showed reduced intensity, while the triple bond region (2300-2150 cm^{-1}) became diminished in As treated samples when compared to the control values suggesting partial masking or involvement of alkyl chains during surface complexation and binding inefficiency of the nitrile or alkyne functional groups to arsenic, respectively. A consistent downfield shift in the carbonyl/Amide I region from 1699-1639 cm^{-1} in controls to approximately 1636-1638 cm^{-1} in treated samples reflected electronic perturbation of conjugated carbonyl and amide functionalities attributable to arsenic coordination. Reduced intensities in the aromatic/NO_2 (1570-1500 cm^{-1}) and alkyl bending (1475-1340 cm^{-1}) regions suggested only minor structural rearrangements at these sites, while persistent bands corresponding to C-N and phenolic O-H vibrations (1369-1314 cm^{-1}) supported their active role in metal binding. The fingerprint region (1162-1030 cm^{-1}), associated with C-O and C-O-C vibrations of ether and alcohol functionalities, remained prominent across all treated samples, identifying these moieties as principal adsorption sites. Emergence and intensification of bands within the 580-400 cm^{-1} region in arsenic-treated samples provided definitive spectroscopic evidence of As-O bond formation, confirming successful arsenic complexation at the cell surface.

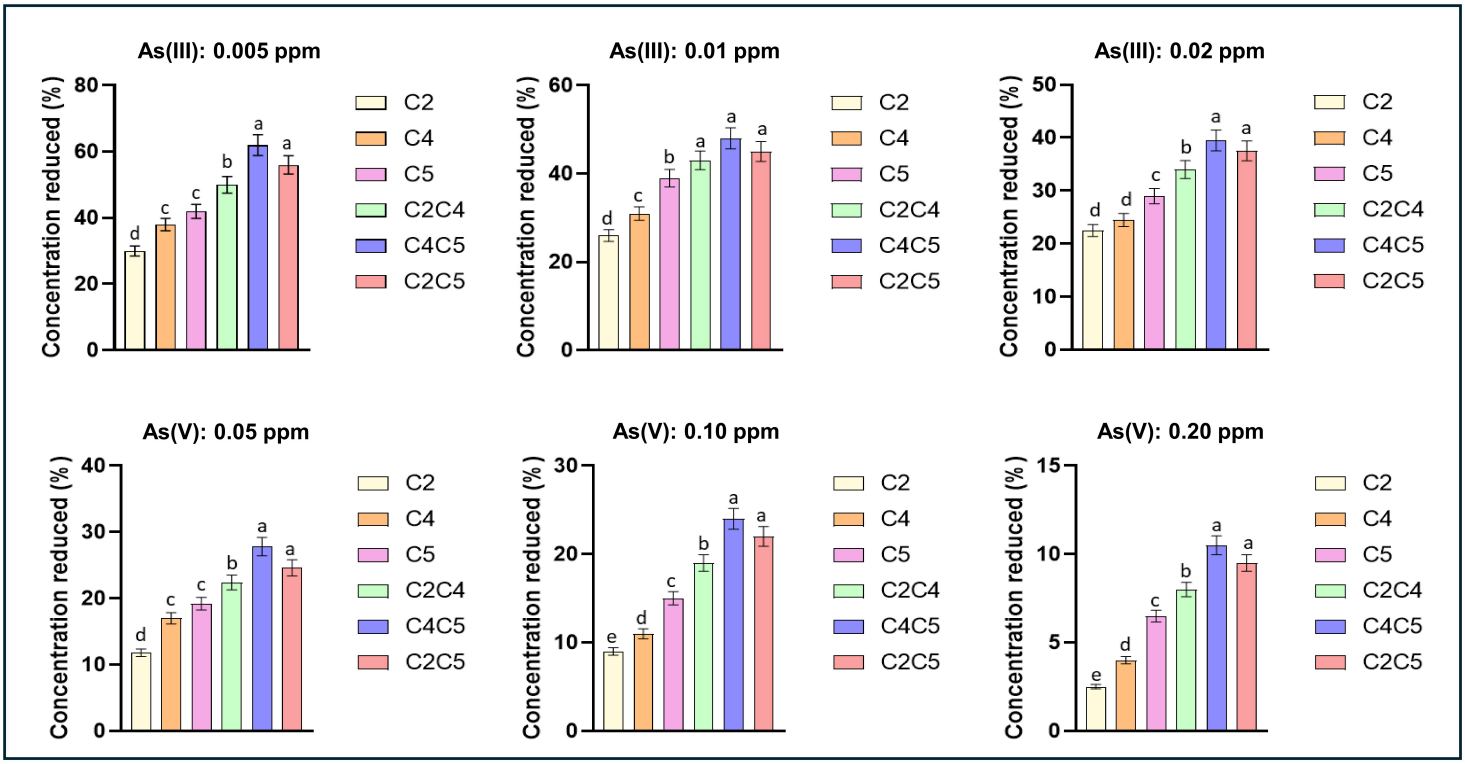


Figure 8

Atomic Absorption Spectroscopy (AAS)-based quantification of arsenic (As; both III and V forms) bioremediation efficiency of isolated bacteria (C2, C4 and C5) and their consortia (C2C4, C2C5 and C4C5). The isolated bacteria (C2, C4 and C5) from arsenic contaminated wastewater and their designed consortia (C2C4, C2C5 and C4C5) profoundly reduced the levels of arsenic in the culture medium within 96 h. Different letters on the error bars indicated significant (p<0.05) differences between the different experimental groups; while same letters indicated no significant different among the experimental groups as revealed from one-way ANOVA followed by a *post-hoc* Duncan's multiple range test (DMRT).

Supplementary Files

This is a list of supplementary files associated with this preprint. Click to download.

- GraphicalAbstract.jpeg
- 1.SupplementaryfileforFigure1Characterization.pptx
- 2.SupplementaryfileforFigure2Biochemicaltests.pptx
- 3.SupplementaryFileforFigure3.zip
- 4.SupplementaryfileforFigure6SEM.pptx
- 5.SupplementaryfileforFigure7FTIR.zip
- 6.SupplementaryfileforFigure8.zip
- SupplementaryTable1.docx